Heart and large vessel interaction in congenital heart disease, assessed by magnetic resonance imaging

Grotenhuis, H.B.

Heynric B. Grotenhuis
Jaap Ottenkamp
Duveken Fontein
Hubert W. Vliegen
Jos J.M. Westenberg
Lucia J.M. Kroft
Albert de Roos

chapter 05

Aortic Elasticity and Left Ventricular Function after Arterial Switch Operation: MR Imaging - Initial Experience.

Radiology. 2008; 249 (3): 801-809.

Abstract

Purpose: To prospectively assess aortic dimensions, aortic elasticity, aortic valve competence and left ventricular (LV) systolic function in patients after the arterial switch operation (ASO) by using magnetic resonance imaging (MRI).

Materials and Methods: Informed consent was obtained from all participants for this local ethics committee - approved study. Fifteen patients (11 male patients, four female patients; mean age, 16 years ± 4 (standard deviation); imaging performed 16.1 years after surgery ± 3.7) and 15 age- and sex-matched control subjects (11 male subjects, four female subjects; mean age, 16 years ± 4) were evaluated. Velocity-encoded MRI was used to assess aortic pulse wave velocity (PWV) and a balanced turbo-field-echo sequence was used to assess aortic root distensibility. Standard velocity-encoded and multisection-multiphase imaging sequences were used to assess aortic valve function, systolic LV function and LV mass. The two-tailed Mann-Whitney U test and Spearman rank correlation coefficient were used for statistical analysis.

Results: Patients treated with the ASO showed aortic root dilatation at three predefined levels (mean difference, 5.7 - 9.4 mm; $P = 0.007$) and reduced aortic elasticity (PWV of aortic arch, 5.1 m/s ± 1.2 vs 3.9 m/s ± 0.7, $P = 0.004$; aortic root distensibility, $2.2*10^{-3}$ mm Hg^{-1} ± 1.8 vs $4.9*10^{-3}$ mm Hg^{-1} ± 2.9, $P < 0.01$) compared with control subjects. Minor degrees of aortic regurgitation (AR) were present (AR fraction, 5% ± 3 in patients vs 1% ± 1 in control subjects; $P < 0.001$). Patients had impaired systolic LV function (LV ejection fraction (LV EF), 51% ± 6 vs 58% ± 5 in control subjects; $P = 0.003$), in addition to enlarged LV dimensions (end-diastolic volume (EDV), 112 ml/m^2 ± 13 vs 95 ml/m^2 ± 16, $P = 0.007$; end-systolic volume (ESV), 54 ml/m^2 ± 11 vs 39 ml/m^2 ± 7, $P < 0.001$). Degree of AR predicted decreased LV EF ($r = 0.41$, $P = 0.026$) and was correlated with increased LV dimensions (LV EDV: $r = 0.48$, $P = 0.008$; LV ESV: $r = 0.67$, $P < 0.001$).

Conclusion: Aortic root dilatation and reduced elasticity of the proximal aorta are frequently observed in patients who have undergone the ASO, in addition to minor degrees of AR, reduced LV systolic function and increased LV dimensions.

Introduction

The arterial switch operation (ASO) has become the preferred method of surgery for transposition of the great arteries (TGA) (1-3). The operation consists of transection and reanastomosis of the aorta and pulmonary trunk above the sinuses, as well as relocation of the coronary arteries (1). Although this technique has substantially reduced the number of sequelae associated with surgical correction of TGA, completion of the ASO may still leave patients with complications such as aortic root dilatation and aortic regurgitation (AR) (1-5).

Aortic wall abnormalities in TGA have been reported that are due to abnormal aorticopulmonary septation, damage to the vasa vasorum, and surgical manipulations during the ASO, predisposing patients to aortic dilatation, aneurysm formation and even aortic dissection (4-7). In addition, aortic distensibility may be reduced by impaired aortic elastogenesis, as well as by scar formation at the site of anastomosis (8,9). Distensibility and pulse wave velocity (PWV) in the aorta have been shown to be markers of vessel wall elasticity, as they are mainly related to the elastic properties of the aorta (10-12).

Both aortic distensibility and aortic dimensions are crucial for aortic valve dynamics. Aortic valve opening occurs in concert with root expansion during the beginning of systole (13,14). Decreased distensibility of the aortic root increases leaflet stress and therefore predisposes for aortic valve dysfunction (14-16). Aortic dilatation contributes to aortic valve dysfunction through loss of coaptation of the aortic valve leaflets (10,17). As a consequence, impaired distensibility and dilatation of the aorta may lead to aortic valve dysfunction and subsequent impairment of left ventricular (LV) function in patients after surgical repair of TGA (10,14-16).

Magnetic resonance imaging (MRI) has been established as an accurate noninvasive tool for assessment of aortic distensibility and PWV (10,12,18-20). To our knowledge, MRI has not previously been used to study the relationship between aortic dimensions, aortic wall elasticity, aortic valve competence and LV function in patients after the ASO. We hypothesized that intrinsic aortic wall dysfunction, as indicated by abnormal distensibility and PWV, in patients after the ASO frequently occurs and that abnormal aortic elastic properties and aortic dilatation may be associated with reduced aortic valve and LV function. Thus, the objective of our study was to prospectively assess aortic dimensions, aortic elasticity, aortic valve competence and LV systolic function in patients after the ASO by using MRI.

Materials and Methods

Patients

The medical ethics committee of Leiden University Medical Center (Leiden, The Netherlands) approved this study and informed consent was obtained from all participants prior to their enrollment in the study. Fifteen patients who had undergone the ASO (mean age, 16 years ± 4 (standard deviation); imaging performed 16.1 years after surgery ± 3.7) and 15 age- and sex-matched healthy control subjects (mean age, 16 years ± 4) were prospectively examined with MRI at our institution. Characteristics of all participants are listed in Table 1. None of the patients who had undergone the ASO used medication.

Table 1. Characteristics of Patients Who Had Undergone the ASO and Healthy Control Subjects .

Characteristics	patients (n = 15)	healthy controls (n = 15)
male / female *	11 (73) / 4 (27)	11 (73) / 4 (27)
age at MRI (years)	16 ± 4	16 ± 4
height (cm)	167 ± 14	168 ± 12
weight (kg)	55 ± 17	60 ± 15
body surface area (m^2) †	1.6 ± 0.3	1.7 ± 0.3
blood pressure systolic (mm Hg)	116 ± 16	121 ± 13
blood pressure diastolic (mm Hg)	66 ± 12	68 ± 11
cardiac frequency (beats per minute)	71 ± 13	69 ± 9
New York Heart Association class (I/ II)	13 / 2	15 / 0
smoking (yes / no)	0 / 15	0 / 15

Note: Unless otherwise indicated, data are means ± standard deviations, with ranges in parentheses. No patient or control subject had a history of smoking.

* Data are numbers of patients, with percentages in parentheses.

† Calculated with the following formula: √ (height (cm) × weight (kg) / 3600).

Twenty-three patients who had undergone the ASO, as reported in our local congenital heart disease database, were initially approached for this study. Inclusion criteria comprised TGA corrected with the ASO, current age between 12 and 25 years, willingness to comply with the study procedures and written informed consent. Exclusion criteria comprised TGA corrected with the Jatene procedure (this procedure includes insertion of an artificial tunnel to connect the right ventricle with the pulmonary artery, creating a different type of configuration of the great arteries) (n = 1), evidence of aortic valve stenosis (aortic velocity > 2.5 m/s at echocardiography) (21), coarctation of the aorta and/or other forms of congenital heart

disease, Marfan syndrome or a family history of Marfan syndrome, repeat ASO or surgery and/or intervention other than the ASO, usage of medication such as beta-blockers and general contraindications to cardiovascular MRI. Seven patients declined to participate for personal reasons. Age- and sex-matched healthy control subjects were selected from our database of individuals with a harmless heart murmur in whom congenital cardiac disease had been excluded in the past with physical examination and echocardiography.

Previously, data in the same patients who had undergone the ASO and control subjects were included in a report on right ventricular function and pulmonary flow analysis (22).

Surgical technique

The ASO was performed in patients with TGA (median age at surgery, 7 days; range, 3 - 21 days) by using cardiopulmonary bypass and moderate hypothermia by one surgeon with 20 years of experience with the ASO. The operation included transection of the aorta above the sinotubular junction and the pulmonary trunk above the pulmonary root, transplantation of the coronary arteries into the root of the pulmonary trunk, switching of the aorta and pulmonary trunk and subsequent reconstruction of the pulmonary trunk with a pericardial patch (Figure 1). The Lecompte maneuver was performed in all 15 patients (23). Associated procedures during the ASO were ventricular septal defect closure in five patients, atrial septal defect closure in six patients and closure of the ductus arteriosus in 10 patients. No perioperative ischemic events were observed.

Figure 1.

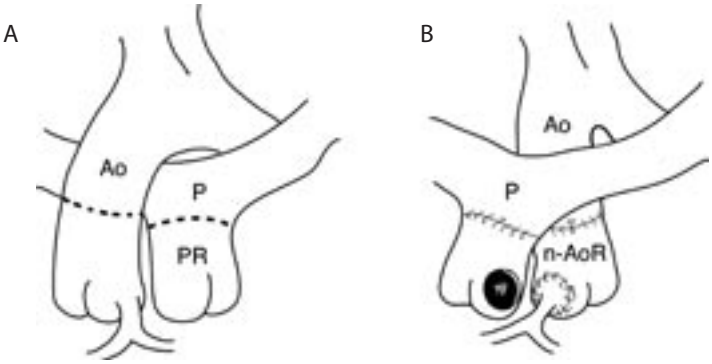

Figure 1a-b. (a) Great artery configuration in TGA before surgical repair. Ao = aorta, P = pulmonary trunk, PR = pulmonary root. **(b)** Great artery configuration after the ASO, which involves transection of the aorta (Ao) above the sinotubular junction and the pulmonary trunk (P) above the pulmonary root, transplantation of the coronary arteries into the root of the pulmonary trunk, switching of the aorta and pulmonary trunk with anterior positioning of the pulmonary trunk (Lecompte maneuver) and subsequent reconstruction of the former aortic root with a pericardial patch. The former pulmonary root has now become the neoaortic root (n-AoR).

MRI

MRI studies were performed with a 1.5-T system (NT 15 Gyroscan Intera; Philips Medical Systems, The Netherlands).

Aortic root dimensions were assessed by using double-oblique transverse images perpendicular to the aorta at the levels of the annulus of the aortic valve, the sinus of Valsalva, the sinotubular junction and the ascending aorta (the latter at the level of the crossing of the right pulmonary artery) (Figure 2) (10). Two sets of orthogonal scout cine images of the aortic root were initially obtained for planning of these acquisition planes. Imaging parameters with the ECG gated steady-state free precession (balanced turbo-field-echo) pulse sequence are listed in (Table 2) (10). Diameter measurements were acquired during diastole, with a trigger delay for all measurements set at 600 ms (10).

Figure 2.

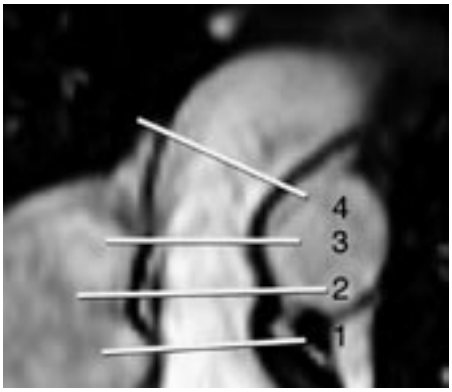

Figure 2. MR image obtained with steady-state free precession cine sequence in 16-year-old healthy male control subject shows four diameter measurements of the aortic root performed at (1) the level of the annulus of the aortic valve, (2) the sinus of Valsalva, (3) the sinotubular junction and (4) the ascending aorta (at the level of the crossing of the right pulmonary artery).

Table 2. MRI Sequence Characteristics.

Sequence	repetition time*	echo time*	gate width*	field of view†	voxel size†	flip angle
Diameter and distensibility measurements	3.2	1.23	34.2	220	1.25×1.25×6.00	50°
Aortic flow measurement	4.8	2.8		300	1.17×1.17× 8.00	20°
Short axis imaging	3.2	1.6	34.2	400	1.60×1.60× 8.00	50°

* expressed in ms.
† expressed in mm.

Aortic distensibility was measured at the level of the sinotubular junction, at the site of anastomosis of the ASO, as previously described (10). Distensibility (in mm Hg^{-1}) is defined by the following equation: $(A_{max} - A_{min}) / (A_{min} \times (P_{max} - P_{min}))$, where A_{max} and A_{min} are the maximal and minimal lumen areas (in square mm) of the sinotubular junction, respectively, and P_{max} and P_{min} are the systolic and diastolic blood pressures (in mm of mercury), respectively (10,12). The minimal lumen area is to be expected early in the cardiac cycle during the isovolumetric contraction phase (just before the beginning of the systolic upslope), while the maximal area is to be expected when the peak of aortic flow passes through the ascending aorta (10). First, the aortic flow was measured just distal to the aortic valve with a velocity-encoded MRI sequence, for timing of the acquisition of the cross-sectional minimal and maximal area measurements. The velocity-encoded sequence was encoded for a fixed velocity-encoding sensitivity of up to 200 cm/s (24). None of the participants showed aliasing on the acquired images, so the velocity-encoded acquisition did not need to be repeated with a higher velocity-encoding sensitivity.

The high temporal resolution (ranging between 7 and 12 ms) enabled optimal timing of the acquisition of the minimal and maximal cross-sectional areas (10). The same acquisition was also used for determination of aortic valve competence (AR fraction) and the measurement of peak flow velocity across the aortic valve. The AR fraction was calculated with the following formula: RV / SFV × 100%, where RV is regurgitant volume in milliliters and SFV is systolic forward volume in milliliters. Minimal and maximal lumen area MRI was subsequently performed after the acquisition planes were manually positioned perpendicular to the aorta at the level of the sinotubular junction at time points of minimal and maximal flow through the aortic root, respectively (10). This approach enabled correction for through-plane motion of the aortic root during contraction. Gate delay was individually applied for optimal timing of the acquisition (10).

Simultaneous blood pressure measurements were noninvasively obtained by using a semiautomatic MRI-compatible sphygmomanometer (Invivo Research, USA) (25).

The PWV of the aorta was measured between the ascending and the proximal descending aorta and between the proximal descending aorta and the abdominal aorta just proximal to the iliac bifurcation (Figure 3). A retrospectively electrocardiographically gated gradient-echo pulse sequence with velocity encoding was applied at the level of the pulmonary trunk to measure through-plane flow in the ascending aorta and proximal descending aorta. A second section was prescribed in the abdominal aorta just proximal to the iliac bifurcation. Imaging parameters were identical to those of the phase-contrast sequence used for timing of the distensibility measurements (18). During MR image acquisition, systolic and diastolic blood pressures were measured as described for the distensibility measurements. PWV was calculated as $\Delta x/\Delta t$ (expressed in meters per second), where Δx is the aortic path length between two imaging levels and Δt is the transit time between the arrival of the foot of the pulse wave at these levels (Figure 3) (18).

Figure 3.

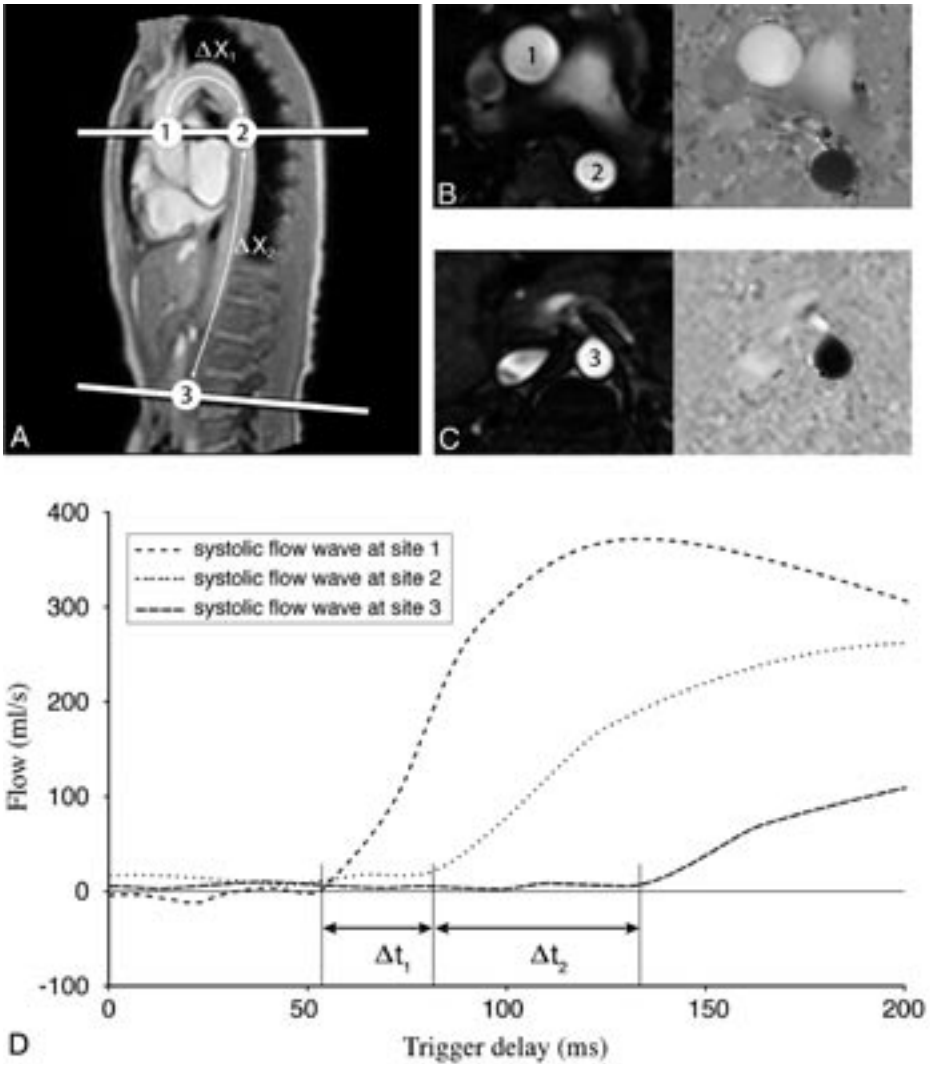

Figure 3 a-d. PWV in the aorta. **(a)** Sagittal MR image shows sites for through-plane velocity-encoded PWV measurements in 16-year-old male healthy control subject: the ascending aorta (1), the proximal descending aorta just distal to the aortic arch (2), and the abdominal aorta just proximal to the iliac bifurcation (3). ΔX_1 = distance between measurement sites 1 and 2, ΔX_2 = distance between measurement sites 2 and 3. **(b,c)** On the corresponding velocity-encoded images, the arrival time of the aortic systolic pulse-wave front can be determined by measuring the through-plane flow. **(d)** Graph shows determination of the arrival times of the three systolic flow waves at the measurement sites. The distance between the sampling sites (derived from **a**) and the transit times (Δt_1 and Δt_2) between the individual arrival times of the systolic flow waves (in **d**) determines the PWV.

Systolic LV function was assessed with a steady-state free precession cine sequence in the short-axis plane by using breath holds. A total of 12 consecutive sections were obtained (40 phases per cardiac cycle) without a section gap (26).

Postprocessing

Diameter and distensibility measurements of the aortic root, as well as systolic LV function images, were analyzed by using the software package MASS (Medis, The Netherlands) (26). LV end-diastolic volume and end-systolic volume were assessed by drawing the LV endocardial contours at end-diastole and end-systole in all sections, as previously described (10,18,26). At end-diastole, the epicardial borders of the LV were drawn to obtain the LV mass with inclusion of the interventricular septum (10,18,26). Indexing was performed according to the Mosteller formula: BSA = $\sqrt{}$ (height (cm) $\times$ weight (kg) / 3600), where BSA is the body surface area in square meters. The following parameters were then determined: end-diastolic volume, end-systolic volume, stroke volume, LV ejection fraction (LV EF) and LV mass (10,26).

Flow velocity - encoded MRI data were analyzed with the software package FLOW (Medis, The Netherlands) (24). Flow curves were obtained with this method for aortic flow during the cardiac cycle. Contours were drawn for the aortic lumen and flow data were subsequently obtained from the velocity data of each voxel in all phases. Peak flow velocity was determined with a time-velocity analysis that revealed the voxel with maximum peak flow throughout the cardiac cycle.

The manual drawing of all MRI contours and analysis of the other results was performed by one researcher (H.B.G., with 3 years of experience in cardiac MRI); these results were subsequently checked by a radiologist (L.J.M.K., with 9 years of experience in cardiac MRI) who was unaware of the patients' conditions.

Statistical analysis

Statistical analysis was performed by using software (SPSS for Windows, version 12.0.1; SPSS, USA). All data are presented as mean $\pm$ 1 standard deviation, unless stated otherwise. The two-tailed Mann-Whitney U test was used to express differences between the patients and control subjects. Correlation between variables was expressed with the Spearman rank correlation coefficient. Linear regression analysis was used to identify predictors of variables with backward elimination procedures. Statistical significance was indicated by $P < 0.05$.

Results

Aortic dimensions and elasticity

Diameters of the aortic root were significantly increased in patients after the ASO as compared with those in the healthy control subjects (Table 3). Dilatation was most pronounced at the level of the sinus of Valsalva, whereas diameters at the level of the ascending aorta were within normal limits. Elasticity of the proximal aorta was found to be reduced, as distensibility at the level of the sinotubular junction was significantly decreased and PWV in the aortic arch was significantly increased in patients after the ASO. PWV in the descending aorta was relatively normal. Aortic dilatation at the level of the sinus of Valsalva was significantly correlated with increased PWV in the aortic arch ($r = 0.36$, $P = 0.049$).

Table 3. Results in 15 Patients Who Had Undergone the ASO and 15 Age- and Sex-matched Healthy Control Subjects .

Parameters	patients	healthy controls	P value mean	difference
diameter annulus (mm)	30.6 ± 5.3	24.3 ± 3.0	0.001	6.3
diameter sinus of Valsalva (mm)	36.4 ± 6.1	27.0 ± 3.6	< 0.001	9.4
diameter sinotubular junction (mm)	29.6 ± 6.0	23.9 ± 2.9	0.007	5.7
diameter ascending aorta (mm)	25.2 ± 5.3	22.6 ± 2.4	0.18	2.6
distensibility (in 10^{-3} mm Hg^{-1}) *	2.2 ± 1.8	4.9 ± 2.9	< 0.01	
PWV aortic arch (m/s)	5.1 ± 1.2	3.9 ± 0.7	0.004	
PWV descending aorta (m/s)	4.1 ± 0.7	3.6 ± 0.3	0.06	
aortic regurgitation fraction (%)	5 ± 3	1 ± 1	< 0.001	
peak-flow velocity at STJ (m/s)	1.63 ± 0.21	1.50 ± 0.32	0.21	
LV EF (%)	51 ± 6	58 ± 5	0.003	
LV EDV (ml/m^2)	112 ± 13	95 ± 16	0.007	
LV ESV (ml/m^2)	54 ± 11	39 ± 7	< 0.001	
LV mass (g/m^2)	49 ± 11	43 ± 12	0.17	

Note: data are expressed as mean ± standard deviation.
* Distensibility was measured at the level of the sinotubular junction.
Abbreviations: ASO = arterial switch operation, PWV = pulse wave velocity, STJ = sinotubular junction, LV = left ventricle, EF = ejection fraction, EDV = end-diastolic volume indexed for body surface area, ESV = end-systolic volume indexed for body surface area.

Aortic Valve Competence

Minor to mild degrees of AR were found in 6 of 15 patients after the ASO, with AR fraction ranging between 5% and 15%. In none of the healthy control subjects did AR fraction exceed

5%. Aortic root dilatation and reduced elasticity of the proximal aorta were associated with the degree of AR, as aortic root dilatation (r ranging between 0.32 and 0.66, $P \leq 0.01$ for all four levels), reduced aortic root distensibility ($r = 0.45$, $P = 0.01$) and increased PWV in the aortic arch ($r = 0.39$, $P = 0.03$) were all correlated with degree of AR fraction. Peak flow velocities across the aortic valve were not increased in our patient group as compared with those in the healthy control subjects (Table 3), supporting the fact that none of the examined individuals had aortic valve stenosis.

LV function

Systolic LV function - expressed by LV EF - was found to be significantly decreased in patients after the ASO as compared with that in the healthy control subjects (Table 3). Linear regression analysis revealed that degree of AR predicted decreased LV EF ($r = 0.41$, $P = 0.026$). LV dimensions (LV end-diastolic volume and LV end-systolic volume) were significantly enlarged in the patient group and were also related to AR fraction ($r = 0.48$, $P = 0.008$ and $r = 0.67$, $P < 0.001$, respectively). Mean LV mass in the patient group was slightly but not significantly larger than that in the healthy control subjects. Mean LV mass was significantly correlated with increased PWV at the level of the aortic arch ($r = 0.48$, $P = 0.008$) and increased LV end-diastolic and LV end-systolic volume ($r = 0.81$, $P < 0.001$ and $r = 0.48$, $P = 0.007$, respectively).

Discussion

Our study revealed aortic root dilatation and reduced elasticity of the proximal aorta, associated with minor degrees of AR, in patients after the ASO. AR was associated with reduced LV systolic function and enlarged LV dimensions in these patients.

Aortic dimensions and elasticity

Patients after the ASO showed dilatation of the aortic root and reduced proximal aortic elasticity as compared with healthy control subjects; these findings are in agreement with those of previous studies (2-5,7). Structural differences between the walls of the two arterial roots have been reported to result in aortic root dilatation and reduced distensibility (7). After the ASO, the former pulmonary arterial wall (the neoaorta after the ASO) is exposed to higher systemic pressures, posing increased stress on the neoaortic wall that may ultimately lead to changes in the structure and function of the neoaortic root. Schoof et al. (27) reported that dilatation was the result of a pulmonary wall adapting to higher systemic pressures. Others have observed structural neoaortic wall abnormalities in patients with TGA even during the neonatal period, suggesting that these wall abnormalities are inherited, analogous to prototypical extremes such as Marfan syndrome and bicuspid aortic

valve disease (5). Whether medial abnormalities of the neoaortic wall are inherent or acquired remains, however, difficult to distinguish (5). Murakami et al. (4) proposed a relationship between neoaortic dilatation and decreased distensibility and damage to the vasa vasorum. The vasa vasorum are a fine network of vessels that supply the outer wall of a larger blood vessel (4). During the ASO, the vasa vasorum are transected and blood flow is inhibited, causing necrosis that may be followed by dilatation and impaired distensibility of the neoaorta (4). Manipulations during the ASO - such as the reimplantation of the coronary arteries - can also lead to changes in the neoaortic root wall that may result in progressive aortic dilatation (7), whereas aortic distensibility may be reduced by impaired aortic elastogenesis, as well as by scar formation at the site of anastomosis (8,9).

Arterial stiffness has been shown to be a cardiovascular risk factor on its own (11). Augmented arterial stiffening is associated with impaired coronary blood flow and LV dysfunction (11). In addition, a strong and independent association has been demonstrated between increased arterial stiffness and the presence of coronary artery disease (28). Therefore, the prognosis of patients with increased arterial stiffness may be worse as compared with healthy control subjects, because numerous other standard risk factors, such as aging, smoking, lipid profiles and sex, act cumulatively over a lifetime (11,28). Early detection of disturbances in arterial stiffness may allow for early therapeutic intervention (29). In patients with Marfan syndrome, beta-blockade has a beneficial effect on the progression rate of aortic dilatation, with reduction of aortic complications (12,25). Whether this is applicable for patients who have undergone the ASO remains to be elucidated.

Aortic Valve Competence

Aortic root dilatation and decreased aortic distensibility are closely related to aortic valve function, with the potential to cause AR (10,18,27,30). Although fewer than half of our patients who had undergone the ASO exhibited minor to mild degrees of AR, dilatation of the aortic root and reduced elasticity of the proximal aorta were found to be significantly correlated with degree of AR. Increased dimensions of the aortic annulus lead to loss of coaptation of the aortic valve leaflets, resulting in varying degrees of central AR (31-33). In addition, aortic valve dynamics are closely related to distensibility of the aortic root. During systole, as the aortic valve opens, the aortic root should expand simultaneously (13,14). Any disturbance in this synchronized process results in increased stress on the aortic valve leaflets (14-16), which will ultimately result in degeneration of the aortic valve leaflets and, consequently, AR.

LV Function

LV systolic function was significantly reduced in our patients after the ASO, despite most patients having New York Heart Association class I cardiac function. LV dysfunction has been suggested to be related to ischemic damage caused by coronary insufficiency or perioperative ischemia. A previous study (3), however, demonstrated no areas of myocardial infarction in patients

after the ASO without ischemic events. As in our patient group, no previous ischemic events were reported, and myocardial scar and coronary imaging were not included in the imaging protocol. In our study, LV dysfunction and increased LV dimensions appeared to be associated with degree of AR, which may be considered as the end point in a sequence of events (30). As a consequence of AR, increased LV mass occurs to maintain normal LV filling pressures (30). A normal LV volume-to-mass ratio is initially maintained, with adequate preservation of LV EF because of the increased preload, but, as AR continues to progress and the LV continues to dilate, increased wall stress may result in LV systolic dysfunction and, consequently, decreased LV EF (30). AR also leads to a volume overload of the LV, hence increasing LV dimensions, which consequently results in decreased LV EF.

Our study had limitations. We used a limited number of patients and control subjects, although the low inter- and intraobserver variability of MRI allows relatively small sample sizes (34). No preoperative or follow-up measurements were available in our observational study, so progression of findings could not be documented. Future longitudinal follow-up studies with larger numbers of patients may further elucidate the predictive value of our findings in patients after the ASO, allowing for multivariate analysis and subgroup analysis, as other parameters may additionally be involved in our findings.

In conclusion, our study revealed aortic root dilatation and reduced elasticity of the proximal aorta in patients after the ASO, in addition to minor degrees of AR, reduced LV systolic function and enlarged LV dimensions. Therefore, despite the fact that the ASO has substantially reduced the number of sequelae associated with surgical correction of TGA, the current findings might pose a prognostic risk for patients after the ASO. Our study showed the feasibility of MRI as an integrated imaging tool for monitoring aortic and LV function parameters, which may facilitate the early detection of aortic and LV dysfunction in patients after the ASO.

References

1. del Nido PJ, Schwartz ML. Aortic regurgitation after arterial switch operation. J Am Coll Cardiol. 2006; 47 (10): 2063-2064.
2. Formigari R, Toscano A, Giardini A, et al. Prevalence and predictors of neoaortic regurgitation after arterial switch operation for transposition of the great arteries. J Thorac Cardiovasc Surg. 2003; 126 (6): 1753-1759.
3. Taylor AM, Dymarkowski S, Hamaekers P, et al. MR coronary angiography and late-enhancement myocardial MR in children who underwent arterial switch surgery for transposition of great arteries. Radiology. 2005; 234 (2): 542-547.
4. Murakami T, Nakazawa M, Momma K, Imai Y. Impaired distensibility of neoaorta after arterial switch procedure. Ann Thorac Surg. 2000; 70 (6): 1907-1910.
5. Niwa K, Perloff JK, Bhuta SM, et al. Structural abnormalities of great arterial walls in congenital heart disease: light and electron microscopic analyses. Circulation. 2001; 103 (3): 393-400.
6. Mersich B, Studinger P, Lenard Z, Kadar K, Kollai M. Transposition of great arteries is associated with increased carotid artery stiffness. Hypertension. 2006; 47 (6): 1197-1202.
7. Hourihan M, Colan SD, Wernovsky G, Maheswari U, Mayer JE Jr, Sanders SP. Growth of the aortic anastomosis, annulus, and root after the arterial switch procedure performed in infancy. Circulation. 1993; 88 (2): 615-620.
8. Hwang HY, Kim WH, Kwak JG, et al. Mid-term follow-up of neoaortic regurgitation after the arterial switch operation for transposition of the great arteries. Eur J Cardiothorac Surg. 2006; 29 (2): 162-167.
9. Verhaaren H, De Mey S, Coomans I, et al. Fixed region of nondistensibility after coarctation repair: in vitro validation of its influence on Doppler peak velocities. J Am Soc Echocardiogr. 2001; 14 (6): 580-587.
10. Grotenhuis HB, Westenberg JJ, Doornbos J, et al. Aortic root dysfunctioning and its effect on left ventricular function in Ross procedure patients assessed with magnetic resonance imaging. Am Heart J. 2006; 152 (5): 975-978.
11. Cruickshank K, Riste L, Anderson SG, Wright JS, Dunn G, Gosling RG. Aortic pulse-wave velocity and its relationship to mortality in diabetes and glucose intolerance: an integrated index of vascular function? Circulation. 2002; 106 (16): 2085-2090.
12. Groenink M, de Roos A, Mulder BJ, Spaan JA, van der Wall EE. Changes in aortic distensibility and pulse wave velocity assessed with magnetic resonance imaging following beta-blocker therapy in the Marfan syndrome. Am J Cardiol. 1998; 82 (2): 203-208.
13. Thubrikar MJ, Heckman JL, Nolan SP. High speed cine-radiographic study of aortic valve leaflet motion. J Heart Valve Dis. 1993; 2 (6): 653-661.
14. Schmidtke C, Bechtel J, Hueppe M, Noetzold A, Sievers HH. Size and distensibility of the aortic root and aortic valve function after different techniques of the Ross procedure. J Thorac Cardiovasc Surg. 2000; 119 (5): 990-997.

15. Thubrikar M, Skinner JR, Aouad J, Finkelmeier BA, Nolan SP. Analysis of the design and dynamics of aortic bioprostheses in vivo. J Thorac Cardiovasc Surg. 1982; 84 (2): 282-290.
16. Thubrikar MJ, Nolan SP, Aouad J, Deck JD. Stress sharing between the sinus and leaflets of canine aortic valve. Ann Thorac Surg. 1986; 42 (4): 434-440.
17. Fedak PW, Verma S, David TE, Leask RL, Weisel RD, Butany J. Clinical and pathophysiological implications of a bicuspid aortic valve. Circulation. 2002; 106 (8): 900-904.
18. Grotenhuis HB, Ottenkamp J, Westenberg JJ, Bax JJ, Kroft LJ, de Roos A. Reduced aortic elasticity and dilatation are associated with aortic regurgitation and left ventricular hypertrophy in nonstenotic bicuspid aortic valve patients. J Am Coll Cardiol. 2007; 49 (15): 1660-1665.
19. Mohiaddin RH, Underwood SR, Bogren HG, et al. Regional aortic compliance studied by magnetic resonance imaging: the effects of age, training, and coronary artery disease. Br Heart J. 1989; 62 (2): 90-96.
20. Bogren HG, Klipstein RH, Mohiaddin RH, et al. Pulmonary artery distensibility and blood flow patterns: a magnetic resonance study of normal subjects and of patients with pulmonary arterial hypertension. Am Heart J. 1989; 118 (5): 990-999.
21. Otto CM, Lind BK, Kitzman DW, Gersh BJ, Siscovick DS. Association of aortic-valve sclerosis with cardiovascular mortality and morbidity in the elderly. N Engl J Med. 1999; 341 (3): 142-147.
22. Grotenhuis HB, Kroft LJ, van Elderen SG, et al. Right ventricular hypertrophy and diastolic dysfunction in arterial switch patients without pulmonary artery stenosis. Heart. 2007; 93 (12): 1604-1608.
23. Lecompte Y, Zannini L, Hazan E, et al. Anatomic correction of transposition of the great arteries. J Thorac Cardiovasc Surg. 1981; 82 (4): 629-631.
24. van der Geest RJ, Niezen RA, van der Wall EE, de Roos A, Reiber JH. Automated measurement of volume flow in the ascending aorta using MR velocity maps: evaluation of inter- and intraobserver variability in healthy volunteers. J Comput Assist Tomogr. 1998; 22 (6): 904-911.
25. Nollen GJ, Groenink M, Tijssen JG, van der Wall EE, Mulder BJ. Aortic stiffness and diameter predict progressive aortic dilatation in patients with Marfan syndrome. Eur Heart J. 2004; 25 (13): 1146-1152.
26. van der Geest RJ, Reiber JH. Quantification in cardiac MRI. J Magn Reson Imaging. 1999; 10 (5): 602-608.
27. Schoof PH, Gittenberger-de Groot AC, de Heer E, Bruijn JA, HazekampMG, Huysmans HA. Remodeling of the porcine pulmonary autograft wall in the aortic position. J Thorac Cardiovasc Surg. 2000; 120 (1): 55-65.
28. Arnett DK, Evans GW, Riley WA. Arterial stiffness: a new cardiovascular risk factor? Am J Epidemiol. 1994; 140 (8): 669-682.
29. Franklin SS. Blood pressure and cardiovascular disease: what remains to be achieved? J Hypertens Suppl. 2001; 19 (3): S3-S8.
30. Bekeredjian R, Grayburn PA. Valvular heart disease: aortic regurgitation. Circulation. 2005; 112 (1): 125-134.
31. Thubrikar MJ, Labrosse MR, Zehr KJ, Robicsek F, Gong GG, Fowler BL. Aortic root dilatation may alter the dimensions of the valve leaflets. Eur J Cardiothorac Surg. 2005; 28 (6): 850-855.

32. Chong WY, Wong WH, Chiu CS, Cheung YF. Aortic root dilation and aortic elastic properties in children after repair of tetralogy of Fallot. Am J Cardiol. 2006; 97 (6): 905-909.
33. Tafreshi RI, Shahmohammadi A, Davari PN. Predictors of left ventricular performance after valve replacement in children and adolescents with chronic aortic regurgitation. Pediatr Cardiol. 2005; 26 (4): 331-337.
34. Bellenger NG, Davies LC, Francis JM, Coats AJ, Pennell DJ. Reduction in sample size for studies of remodeling in heart failure by the use of cardiovascular magnetic resonance. J Cardiovasc Magn Reson. 2000; 2 (4): 271-278.